Supporting information for:

Exploring Environment-dependent effects of Pd nanostructures on reactive oxygen species (ROS) using electron spin resonance (ESR) technique: implications for biomedical applications

Tao Wen,[a, b, d] Weiwei He,[b, c] Yu Chong,[b] Yi Liu,[b] Jun-Jie Yin*[b] and Xiaochun Wu*[a]

[a] CAS Key Laboratory of Standardization and Measurement for Nanotechnology, National Center for Nanoscience and Technology, Beijing 100190, P. R. China.

[b] Division of Analytical Chemistry, Office of Regulatory Science, Center for Food Safety and Applied Nutrition, US Food and Drug Administration, College Park 20740, MD, USA.

[c] Key Laboratory of Micro-Nano Materials for Energy Storage and Conversion of Henan Province, Institute of Surface Micro and Nano Materials, Xuchang University, Henan 461000, P. R. China

[d] University of the Chinese Academy of Sciences, Beijing 100190, P. R. China.

*Corresponding author.

E-mail address: wuxc@nanoctr.cn, junjie.yin@fda.hhs.gov

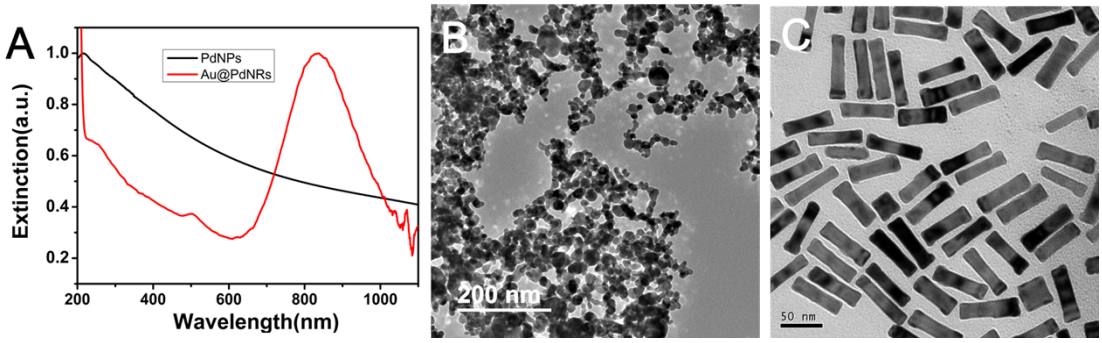

Fig. S1 (A) UV-Vis spectra and typical TEM images for (B) Pd NPs, and (C) Au@Pd NRs.

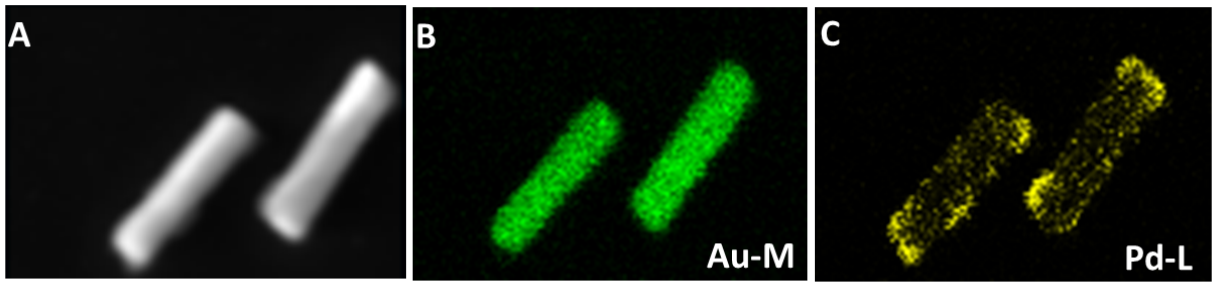

Fig. S2 (A) STEM-HAADF images and STEM-EDX element maps of (B) Au and (C) Pd for Au@Pd NRs.

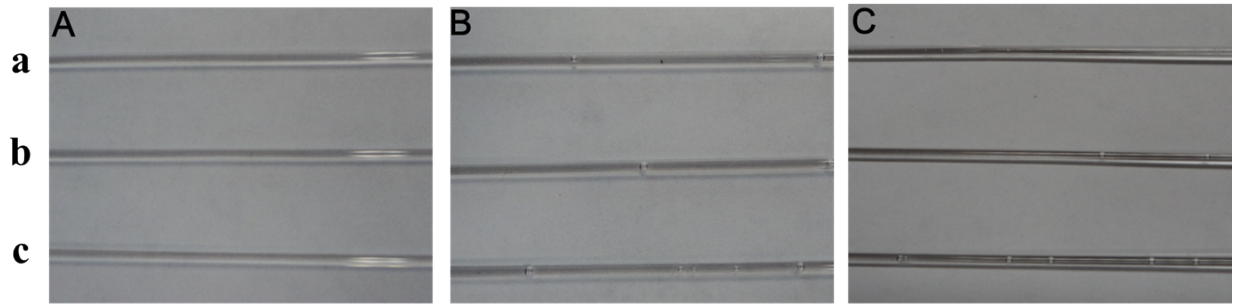

Fig. S3 Observation of the dioxygen bubbles generated at 15 min in samples containing 5 mM H_2O_2 and (A) none, (B) 2.5 μg/mL Pd NPs, (C) 2.5 nM Au@Pd NRs. The pH values were (a) 7.4, (b) 9.4, and (c) 10.9.

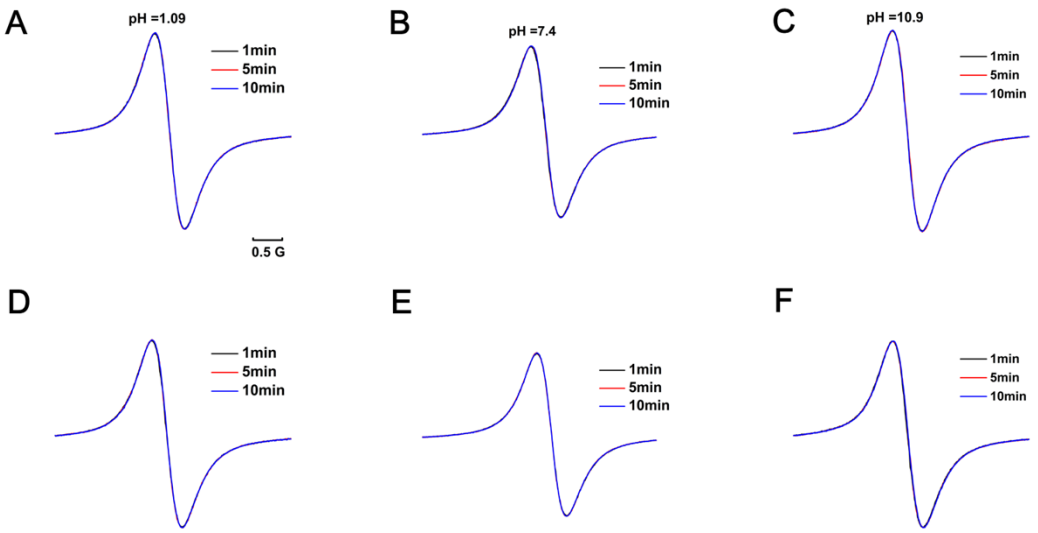

Fig. S4 ESR spectra of samples in the absence (A-C) and presence (D-F) of 5 mM H_2O_2. Solutions contained 0.2 mM ^{15}N-PDT, and 10 mM buffer with different pH values: (A, D) pH 1.09, (B, E) pH 7.4, (C, F) pH 10.9.

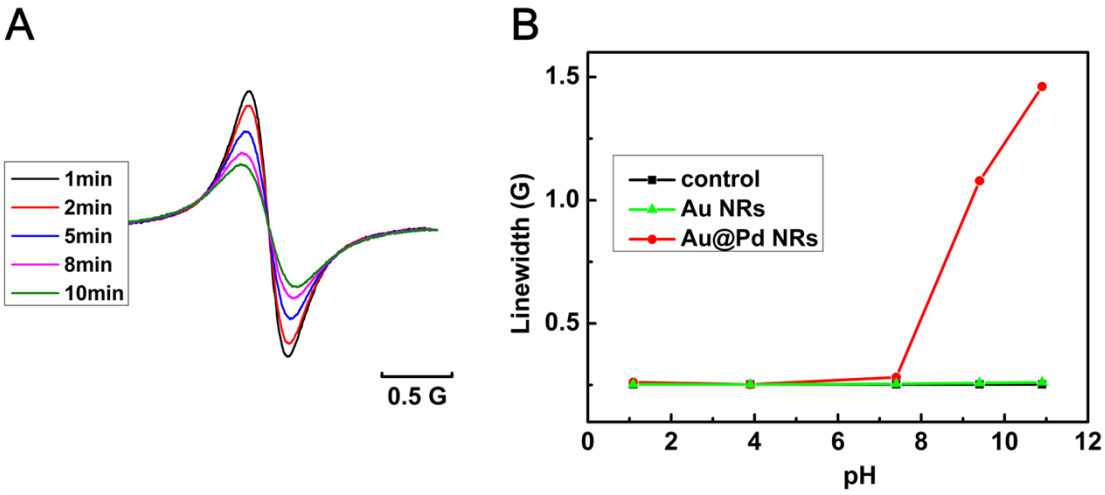

Fig. S5 (A) ESR spectra of ^{15}N-PDT in the presence of Au@Pd NRs, buffer (pH 7.4), and H_2O_2 at different time intervals. (B) Effect of pH on linewidth for NRs after incubation for 1 min. The solutions contain 10 mM buffer, 0.2 mM ^{15}N-PDT, 5 mM H_2O_2 and 2.5 nM NRs.

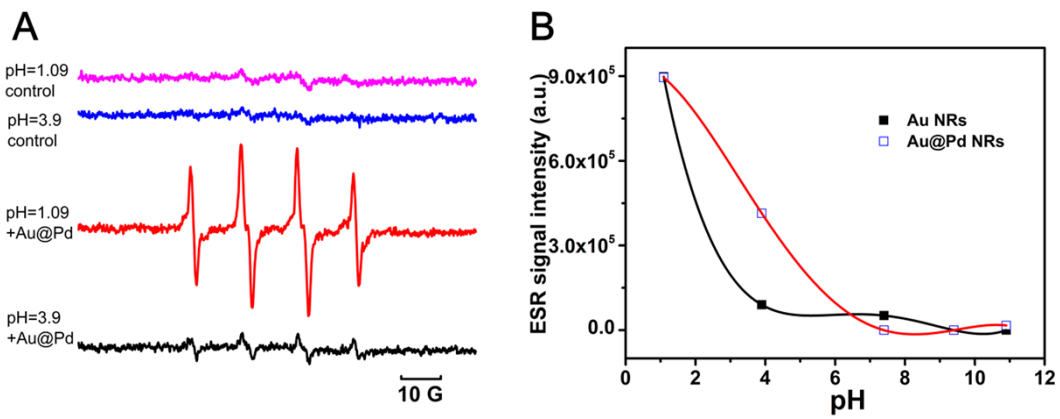

Fig. S6 (A) ESR spectra of BMPO/•OH adducts in the absence and presence of 2.5 nM Au@Pd NRs. Samples contain 10 mM buffer (pH 1.09 or pH 3.9), 5 mM H_2O_2, 25 mM BMPO. (B) Effect of pH on the generation of •OH. The solutions contain 25 mM BMPO, 5 mM H_2O_2, 10 mM different pH buffer and 2.5 nM NRs. ESR spectra were collected after 1 min of incubation and averaged from 9 scans.

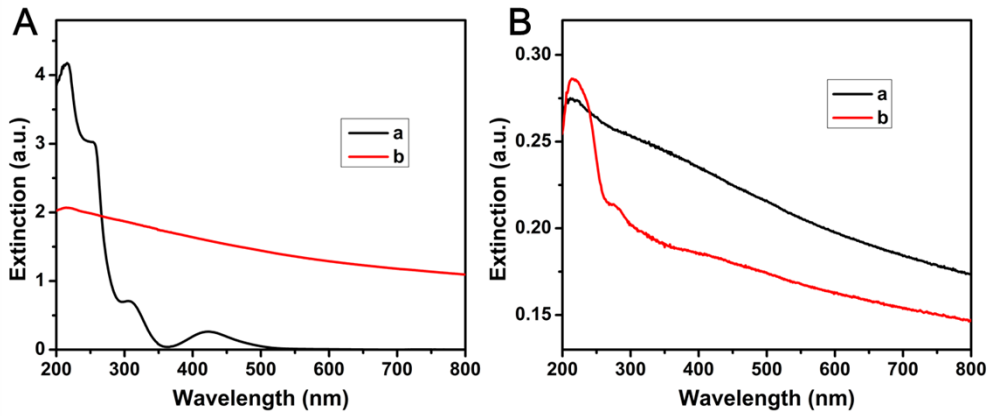

Fig. S7 (A) UV-Vis spectra of (a) 2.5 mM K_2PdCl_4, (b) 100 μg/mL Pd NPs (1 mM) in water. (B) Difference of UV-Vis spectra in the presence and absence of 20 μg/mL Pd NPs and reaction for (a) 0 min and (b) 60 min. Sample solutions contain 10 mM buffer (pH 1.09) and 1 mM H_2O_2.

To investigate the possible mechanism for the generation of •OH in the presence of Pd NPs, we measured the UV-vis extinction spectra of Pd NPs before and after reacting with H_2O_2. Owing to poor dispersibility, Pd NPs solutions show strong scattering and give a gradually increased scattering signal from 800 nm to short wavelength regions (Fig. S7 A). To observe the change after reaction, we obtained the difference of UV-Vis spectra in the presence and absence of 20 μg/mL Pd NPs before and after reaction for 1 h in 1 mM H_2O_2 and 10 mM buffer (pH 1.09). After the decomposition of H_2O_2 in buffer from Pd NPs and H_2O_2 in buffer, we obtained a qualitative view of reaction products from the change in UV-vis spectra. As Fig. S7 B shows, a spectrum similar to that of Pd^{2+} ions was clearly visible after decomposition of H_2O_2 for 1 h in the presence of Pd NPs. Data obtained from ICP-MS analysis of the supernatant shows the existence of Pd^{2+} ions after reaction for 1 h (data not shown). It is well known that both the oxygen and H_2O_2 have high oxidation abilities under acidic conditions, which can be evidenced from their reduction potential:

$$O_2 + 4\ H^+ + 4\ e^-\ \ 2\ H_2O\ (+1.229\ V)$$

$$H_2O_2 + 2\ H^+ + 2\ e^-\ \ 2\ H_2O\ (+1.78\ V)$$

Thus, we propose that Pd NPs were oxidized to Pd^{2+} (Pd^{2+}/Pd = + 0.951 V) in the present of H_2O_2 under acidic condition:

$$Pd + H_2O_2 + 2\ H^+\ \ Pd^{2+} + H_2O$$

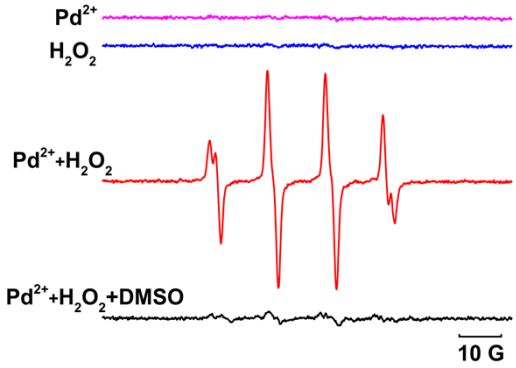

Fig. S8 ESR spectra of BMPO/•OH adducts obtained from samples containing 25 mM BMPO. ESR spectra were collected after 3 min of incubation. [K_2PdCl_4] = 2.5 mM, [H_2O_2] = 5 mM, and [DMSO] = 10%.

In the presence of Pd^{2+}, •OH can be generated during decomposition of H_2O_2. A BMPO/•OH signal is not observed from controls (Fig. S8). However, the solution has a strong BMPO/•OH signal in the presence of Pd^{2+} (Fig. S8). Again, adding 10% DMSO reduces signal significantly. As reported in previous research, hydrogen peroxide can produce •OH mainly in two ways: 1) using UV irradiation, and 2) Fenton or Fenton-like reactions involving transition metal ions such as Fe^{2+} and Cu^{2+}.[S1] Herein, we suppose the generation of •OH by Pd NPs under acidic condition is mainly attributed to Pd^{2+}, formed in a reaction with H_2O_2, and a subsequent Fenton-like reaction ($Pd^{2+} + 2\ H_2O_2 \rightarrow Pd^{4+} + 2\ \bullet OH + 2\ OH^-$).

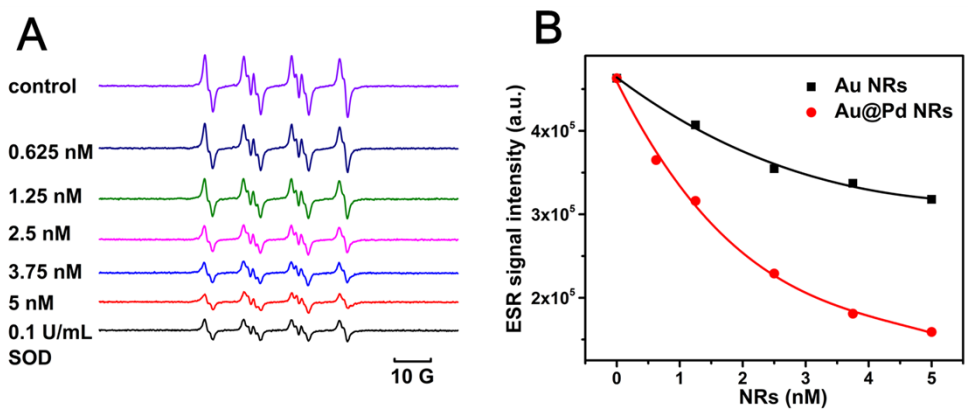

Fig. S9 SOD-like activity of Au NRs and Au@Pd NRs in scavenging superoxide under neutral conditions in Xan/XOD system. (A) ESR spectra of BMPO/•OOH adducts obtained from samples containing different concentration of Au@Pd NRs or SOD in Xan/XOD system. (B) Concentration effect on $O_2^{\bullet-}$ scavenging activity of Au NRs and Au@Pd NRs. Xan/XOD system contains 1 mM Xan, 0.05 U/mL XOD, 0.05 mM DTPA, and 10 mM PBS buffer (pH 7.4). ESR spectra were collected after incubation with 25 mM BMPO for 5 min.

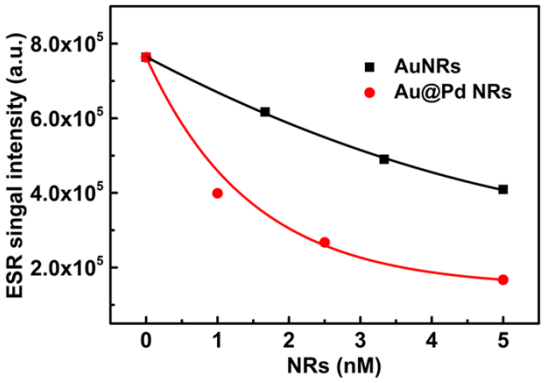

Fig. S10 Concentration effect on singlet oxygen scavenging activity of Au NRs and Au@Pd NRs in ZnO nanoparticles (0.02 mg/mL) system. ESR spectra were collected after irradiation for 1 min containing 10 mM TEMP.

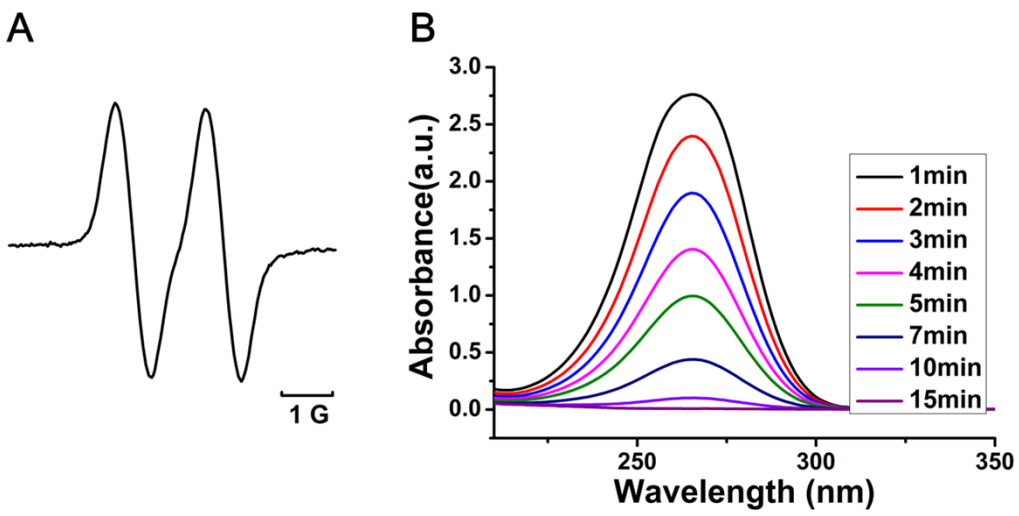

Fig. S11 (A) ESR spectrum of ascorbyl radical. (B) Evolution of UV-Vis spectra for a sample containing 2 U/mL AAO and 5 mM AA in 10 mM PBS (pH 7.4).

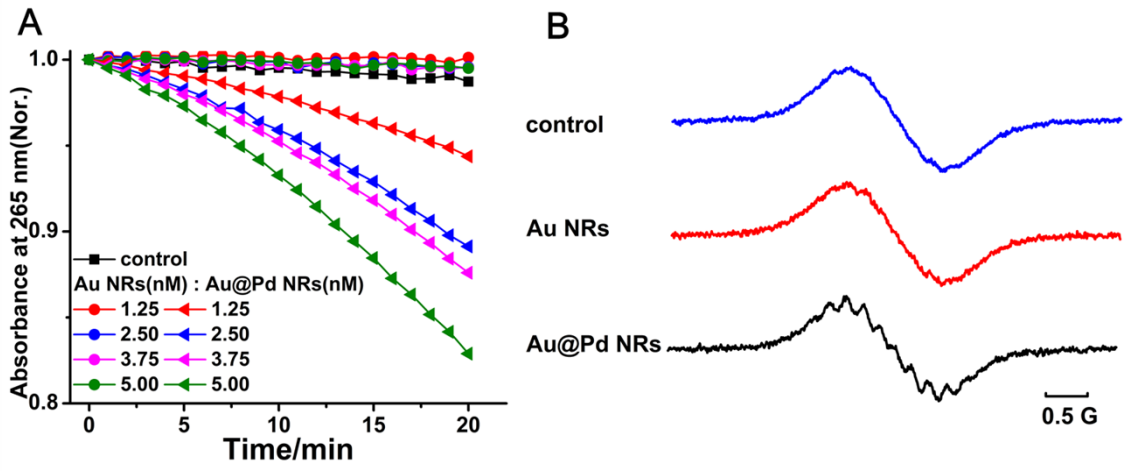

Fig. S12 Catalytic activity of NRs during oxidation of AA. (A) AA absorbance at 265 nm as a function of time with different concentrations of Au NRs and Au@Pd NRs. UV-Vis spectra for solutions of NRs with 0.25 mM AA in 10 mM PBS (pH 7.4). (B) ESR spectra for samples containing CTPO and NRs after mixing 5 min. The concentrations are: [CTPO] = 100 μM, [NR] = 2.5 nM, [AA] = 5 mM, and [PBS] = 10 mM.

Effect on CPH

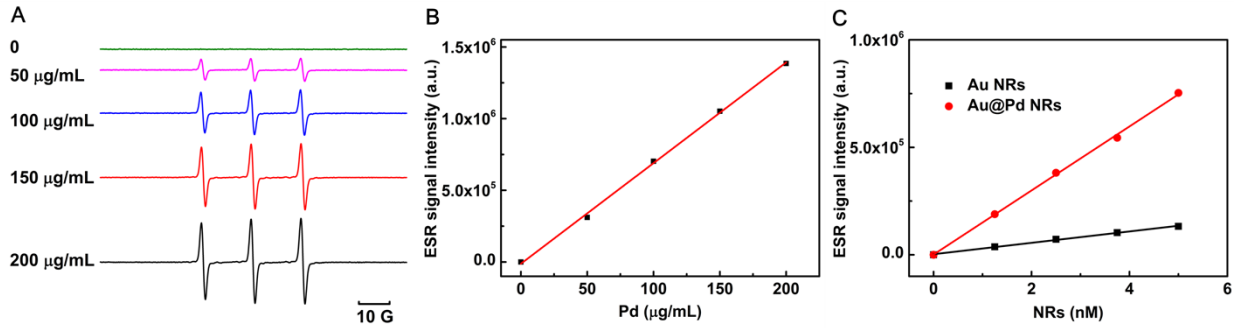

Fig. S13 Catalytic role of Pd NSs on CPH oxidation. (A) ESR spectra of CP• obtained from samples containing 100 μM CPH, and different concentration of Pd NPs. Effects of (B) Pd NPs and (C) NRs concentration on ESR signal intensity. ESR spectra were collected after incubation for 3 min. [CPH] = 100 μM.

We use 1-Hydroxy-3-carboxy-2,2,5,5-tetramethylpyrrolidine- hydrochloride (CPH) as an ESR probe to demonstrate the catalytic role of NSs acting as an oxidase mimic. CPH, itself, is ESR silent, but can be oxidized to form CP-nitroxide radicals (CP•) which show a characteristic ESR signal having three lines with intensity ratios of 1:1:1 (Fig. S13A).[S2] We observe nearly linear concentration-dependence in CP• intensity from solutions containing CPH and Pd NSs (Fig. S13B and S13C). Both Pd NPs and Au@Pd NRs show catalytic activity on CPH oxidation. Compared to Au NRs, Au@Pd NRs show an enhanced activity for catalyzing the oxidization of CPH at same particle concentration, indicating that Pd is better than Au in catalyzing CPH oxidation by oxygen molecules.

References

S1 W. He, Y. T. Zhou, W. G. Wamer, M. D. Boudreau and J. J. Yin, *Biomaterials*, 2012, **33**, 7547-7555.

S2 T. Gordonov, E. Kim, Y. Cheng, H. Ben-Yoav, R. Ghodssi, G. Rubloff, J.-J. Yin, G. F. Payne and W. E. Bentley, *Nat. Nanotechnol.*, 2014, **9**, 605-610.